Progress In Electromagnetics Research Letters, Vol. 109, 41–48, 2023

Three 24 GHz End-Fire Dipole Antennas

Yanfei Mao[1, 2], Chungeng Zhu[1, 2], Shiju E[1, 2, *], and Jiancheng Cai[1, 2]

Abstract—An end fire antenna architecture based on transmission line (TML) theory is suggested. N element end fire antenna array could be constructed with $N-1$ elements of full wave dipole antennas and one half wave dipole antenna without additional impedance matching network. The N dipole antennas are placed with each other with a distance of quarter wave length, while the one half wave dipole antenna is at the outermost of the array, the farthest from the feeding point of the antenna array. And three 24 GHz dipole end-fire antenna arrays with gains of 7.1, 8.4, and 9.4 dB respectively are presented to explain and verify this end fire antenna architecture based on transmission line theory. Simulation and measurement results of the three end-fire antennas are given and compared. This 24 GHz end-fire antenna architecture could be utilized in 24 GHz planar end-fire antenna arrays to increase the effective isotropic radiated power (EIRP) of the transmitter.

1. INTRODUCTION

For RF system, one difficult task is to design high output power transmitters. High output power amplifiers or doublers and high gain antenna helps to improve the EIRP of the transmitter. High output power amplifiers or doublers are not in the scope of the paper. According to [1], both directivity (D) and half power beam width (HP) of end fire array are twice of the broadside array. Therefore, this paper focuses on end fire array antenna and presents an end fire antenna architecture based on transmission line theory.

Many studies have been carried out on dipole end-fire antennas. In [2], a 24 GHz cavity-backed end-fire dipole antenna with a gain of 8.17 dB based on a substrate-integrated suspended line (SISL) platform is given. A 24 GHz end fire dipole antenna with a gain of 5.8 dB for phase arrays and multiple-input multiple-output (MIMO) is obtained in [3]. In [4], a 2.4 GHz low-profile wideband circularly polarized (CP) magnetoelectric (ME) antenna with a gain of 7.57 dB and an end-fire radiation beam is proposed. In [5], a 24 GHz wideband vertically-polarized end-fire magneto-electric (ME) dipole antenna with a gain of 6.9 dB is presented. A novel 24 GHz wideband microstrip-fed end-fire magneto-electric (ME) dipole antenna element with a gain of 5.3 dB is proposed in [6]. In [7], a 24 GHz three-element dipole end-fire antenna composed of half wave dipole antennas with a gain of 8.8 dB is given. In [8], a 24 GHz helix end-fire antenna with high gain turn ratio (with a gain of 9.3 dB at 24 GHz) is presented. In [9], concepts of log-periodic dipole antenna arrays are discussed. In [10], a printed log-periodic dipole array antenna without director cell with a gain of 9.5 dB is given, and for comparison, a printed log-periodic dipole array antenna using a director cell is presented with a gain of 11 dB.

Received 28 November 2022, Accepted 7 February 2023, Scheduled 19 February 2023

* Corresponding author: Shiju E (eshiju@163.com).

[1] Engineering College, Zhejiang Normal University, City of Jinhua, Zhejiang Province, China. [2] Key Laboratory of Urban Rail Transit Intelligent Operation and Maintenance Technology and Equipment of Zhejiang Province, Zhejiang Normal University, Jinhua 321000, China.

2. MATHEMATICAL FORMULATION, DETAILS OF THE DESIGN PROCEDURE AND THE TML METHOD

An end-fire antenna based on TML theory is given in this paper. Fig. 1 shows the circuit model of an N element end fire antenna array. N element end fire antenna array could be constructed with $N-1$ elements of full wave dipole antennas, $Z_2 \sim Z_N$ and one half wave dipole antenna Z_1. The N dipole antennas are placed with a distance of transmission line quarter wave length from each other, while the half wave dipole antenna Z_1 is at the outermost of the array, the farthest from the feeding point of the antenna array. Impedance of half wave dipole antenna Z_1 is almost equal to characteristic impedance of the transmission line $Z_{1i} = Z_0 = Z_1 = R_L$, and impedance matching is achieved at the load. Impedance of the full wave dipole antenna Z_2 is almost equal to R_∞, $Z_2 = R_\infty$ and is connected in parallel with Z_0. According to the formula of total impedance Z_{tot} of two parallel impedances Z_0 and R_∞, $Z_{2i} = Z_{tot} = Z_0 || R_\infty \approx Z_0$. Therefore, connecting full wave dipole antennas Z_2 in parallel in the circuit will not affect the impedance matching of the antenna array. With the same reasoning, we could obtain that $Z_{(N-1)i} \approx Z_{(N-2)i} \approx Z_{2i} \approx Z_{1i} \approx Z_0 = 50\,\text{Ohm}$. Impedance matching is achieved throughout the whole circuit in a natural way.

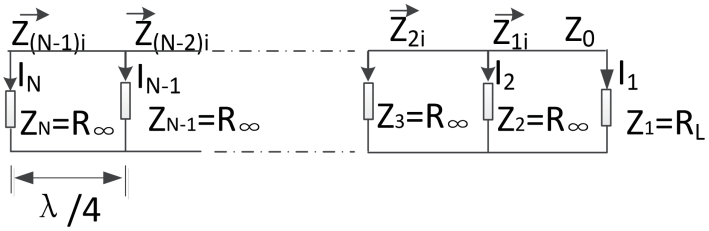

Figure 1. Circuit model of an N-element end fire antenna architecture based on transmission line theory.

In order to clearly illustrate the principle of the dipole antenna array, Fig. 2 shows a prototype of a 4-element end fire antenna architecture based on transmission line theory. Fig. 3 gives the circuit model of the 4 element end fire antenna array. Impedance of the half wave dipole antenna is matched to the characteristic impedance of transmission line Z_0 50 Ohm. Impedance of the arm of full wave dipole antenna could be regarded as R_∞; therefore, it will not affect the impedance matching of the antenna array at all. $Z_{1i} \approx Z_{2i} \approx Z_{3i} \approx Z_0 = 50\,\text{Ohm}$. No additional matching network is required for this end fire antenna array, and its structure is very simple.

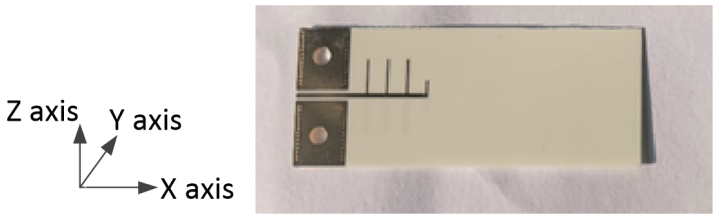

Figure 2. Prototype of a 4-element end fire antenna architecture based on transmission line theory.

According to current division rule of parallel circuits, ratio of currents of the four dipoles is as follows: $i_1 : i_2 : i_3 : i_4 : i_n = 1 : \frac{50}{R_\infty} : \frac{50}{R_\infty}(1 + \frac{50}{R_\infty}) : \frac{50}{R_\infty}(1 + \frac{50}{R_\infty})^2 : \frac{50}{R_\infty}(1 + \frac{50}{R_\infty})^{n-2}$. According to simulation results in HFSS, an estimated value for R_∞ is obtained, $R_\infty \approx 400$, and we take the 4-element end-fire antenna as an example. Therefore, pattern function of the 4-element end-fire array is shown as the following equation. $\frac{\cos(\pi \cos\theta)+1}{\sin\theta}$ is the gain pattern of full-wave dipole antenna, while

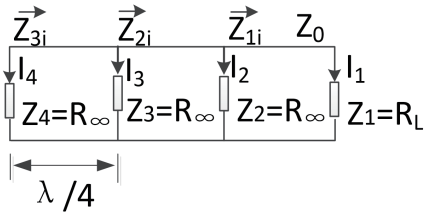

Figure 3. Circuit model of the 4 element end fire antenna architecture.

$\frac{\cos(\frac{\pi}{2}\cos\theta)}{\sin\theta}$ is the pattern of half wave dipole antenna.

$$f(\theta)=\frac{\cos(\pi\cos\theta)+1}{\sin\theta}\left(e^{-j\frac{3\pi}{2}\cos\theta}+\frac{0.14}{0.158}e^{-j\frac{\pi}{2}}e^{-j\pi\cos\theta}+\frac{0.125}{0.158}e^{-j\frac{\pi}{2}\cos\theta}e^{-j\pi}\right)+\frac{\cos\left(\frac{\pi}{2}\cos\theta\right)}{\sin\theta}\frac{1}{0.158}e^{-j\frac{3}{2}\pi} \quad (1)$$

3. SIMULATION AND MEASUREMENT RESULTS

Three end fire antenna arrays are designed to verify the end fire antenna topology: 2-element end fire antenna array, 3-element antenna array, and 4-element antenna array. Fig. 4 shows the prototype of the three antenna arrays.

Design parameters of the antennas in Fig. 4 are as follows: half of full transmission line wave length $L1$ is 4.7 mm; quarter transmission line wave length $L2$ is 2.4 mm; distances between full wave

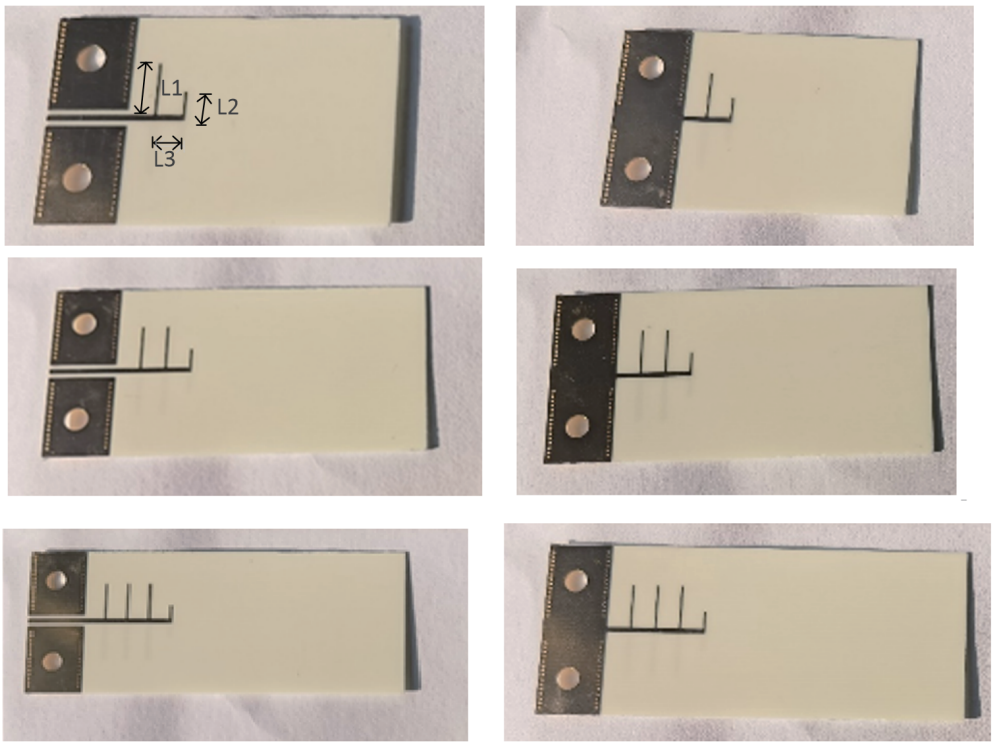

Figure 4. Prototype of three 24 GHz end-fire antennas, top view and bottom of 2-element end fire dipole antenna array, 3-element end fire dipole antenna array and 4-element end fire dipole antenna array.

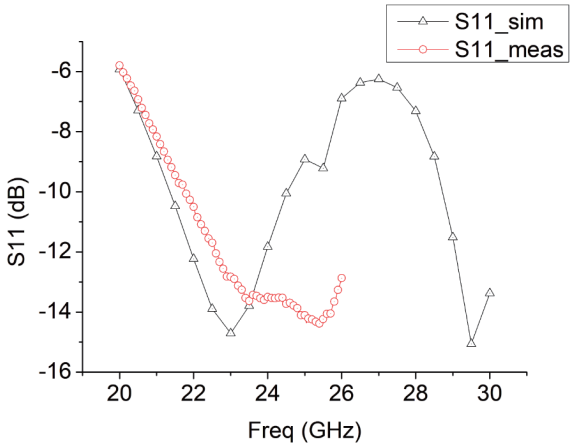

Figure 5. S parameter of the 2-element end fire dipole antenna array.

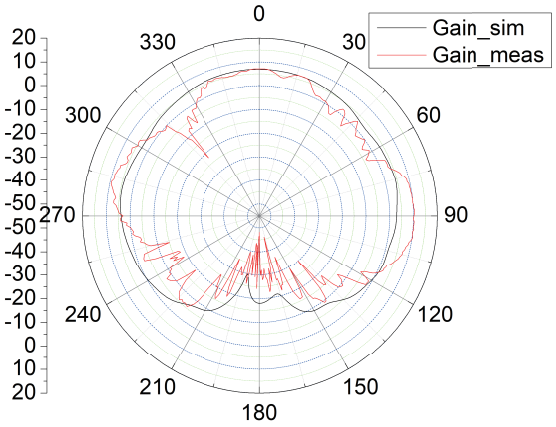

Figure 6. Gain in x-y plane of the 2-element end fire dipole antenna array.

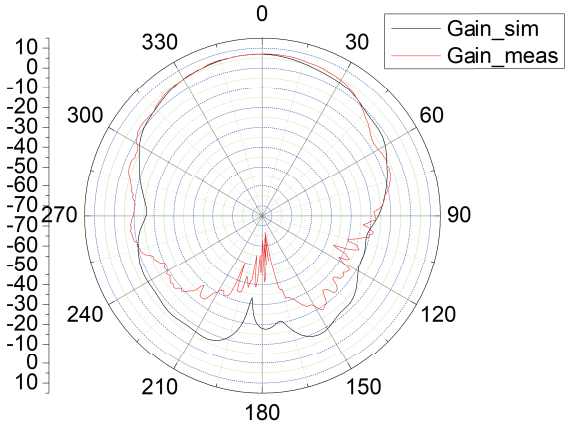

Figure 7. Gain in x-z plane of the 2-element end fire dipole antenna array.

transmission lines and half wave transmission line $L3$ are 2.1 mm. Thickness of the substrate Roger 4350 is 0.254 mm.

Figures 5, 6, and 7 show the simulated and measured antenna gains and S_{11} performances of the two-element end-fire antenna array. Fig. 8, Fig. 9, and Fig. 10 show the simulated and measured antenna gains and S_{11} performances of the three-element end-fire antenna array. Fig. 11, Fig. 12, and Fig. 13 show the simulated and measured antenna gains and S_{11} performances of the four-element end-fire antenna array. Measurement results agree with the simulation ones. The 2-element, 3-element, 4-element end fire dipole antenna arrays achieve the maximum gains of 7.1 dB, 8.4 dB, and 9.4 dB, half power bandwidths of 71°, 44°, and 38° in x-y plane, and half power bandwidths of 47°, 66°, and 59° in x-z plane, respectively. Measured cross polarization is -20 dB, -28 dB, and -28 dB respectively for the three antennas. Measured S_{11} bandwidths of the three antennas are $>$ 4.25 GHz, $>$ 5.25 GHz, and $>$ 5.1 GHz respectively because the network analyzer Ceyear 3672B can only measure up to the frequency of 26 GHz. Also, due to pandemic of corona virus, a Qualwave 2.92 mm end launch connector is utilized to measure the antennas rather than Southwest end launch connector.

The three 24 GHz antennas are measured in the Key Laboratory of RF Circuits and System Ministry of Education, School of Electronics and Information, Hangzhou Dianzi University, for measurements of S parameter, gain, and radiation pattern of the antennas. A microwave and millimeter wave anechoic chamber, with a total area about 150 square meters, was built in 2021, relying on the key laboratory of the Ministry of Education for RF Circuits and Systems of Hangzhou University of Electronic Science

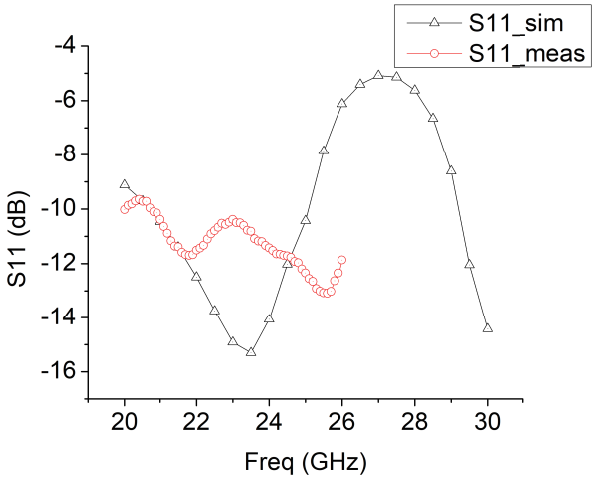

Figure 8. S parameter of the 3-element end fire dipole antenna array.

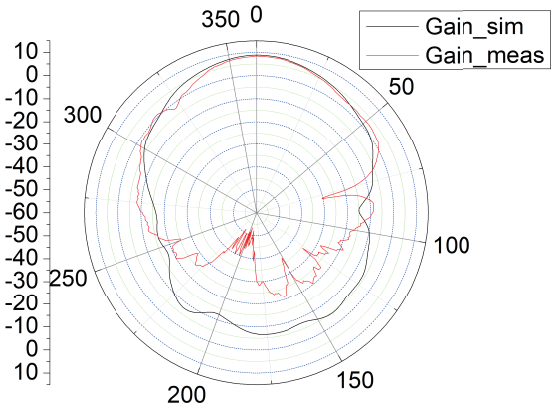

Figure 9. Gain in x-y plane of the 3-element end fire dipole antenna array.

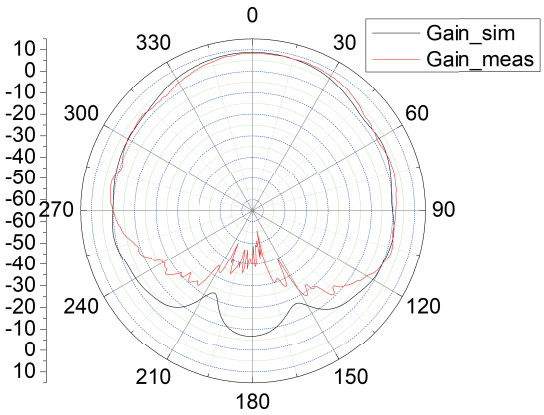

Figure 10. Gain in x-z plane of the 3-element end fire dipole antenna array.

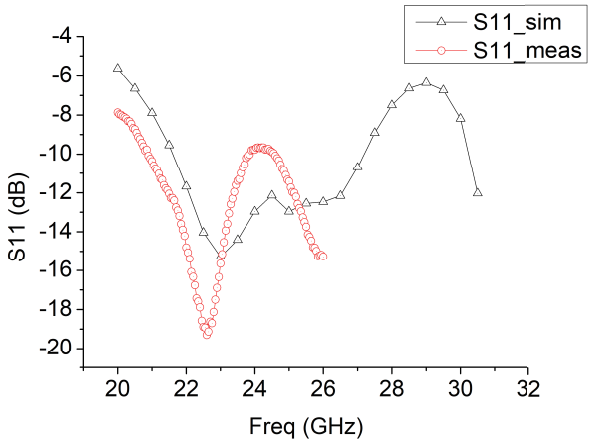

Figure 11. S parameter of the 4-element end fire dipole antenna array.

and Technology. The laboratory is equipped with testing equipment such as vector network, control switchboard, and scanning table, which covers multiple polarization far field gain pattern testing within 110 GHz and near-field plane/cylinder electric field distribution scanning testing. A vector network 3672C, standard gain horn working in the band of 18 $\sim$ 26.5 GHz, a low noise amplifier 3840F, a data measurement controller 3643K, a customized turntable/scanning table, and a customized control switchboard are utilized to measure the 24 GHz dipole antennas in the paper.

4. MORE DISCUSSIONS ON END-FIRE ANTENNA

Table 1 gives a comparison of this work with state of the art. Compared with antennas in [2, 3, 5–7, 11], with the same number of dipole antenna units, the end-fire dipole antenna array in this work has comparable antenna gain at 24 GHz, and by utilizing transmission line theories, end-fire antenna arrays in this work are simpler in design (simplicity in structure and without additional impedance matching networks). Compared with antenna array in [2], the antenna in [2] has a much more complicated design (with 10 metal layers and 5 substrate layers) to realize impedance matching. Compared with the antenna in [3], the antenna in [3] utilizes an additional director to enhance the gain. Compared with the antenna in [7], the matching method in this work is different. Both full wave dipole and half wave dipole are utilized to realize impedance matching, and this end fire architecture is well suitable for N-element end fire dipole antenna array ($N \geq 2$). Compared with the antenna in [10], the matching method in this work is also different. The width and distances of neighboring dipole units in [9, 10] are

Table 1. Comparison state of the art.

	Freq (GHz)	Gain (dBi)	Number of dipole antenna units	topology
[2]	24	8.17	2	Cavity-backed end-fire dipole antenna
[3]	24	5.8	2	5G end-fire elements with a pair of dipoles
[5]	24	6.9	2	End-fire ME dipole antenna
[6]	24	5.3	2	ME dipole end-fire antenna
[7]	24	8.8	3	3-element end fire dipole antenna
[10]	32	9.5/11	4	4-element end fire dipole antenna
[11]	0.5–6	6	6	printed Log-Periodic antenna
[12]	0.4, 0.9, 1.8	6	1	an integrated multifunction antenna
This work	24	7.1	2	2-element dipole end-fire antenna
This work	24	8.4	3	3-element dipole end-fire antenna
This work	24	9.4	4	4-element dipole end-fire antenna

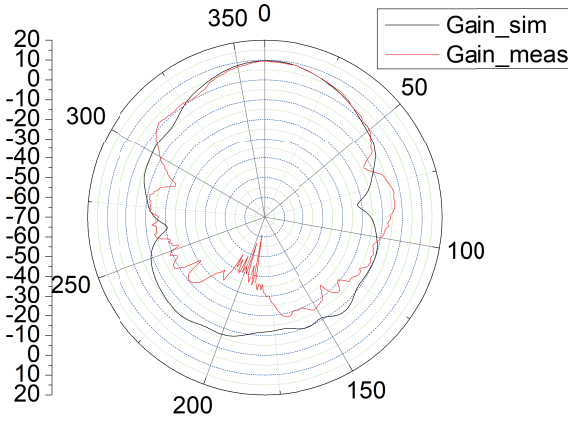

Figure 12. Gain in x-y plane of the 4-element end fire dipole antenna array.

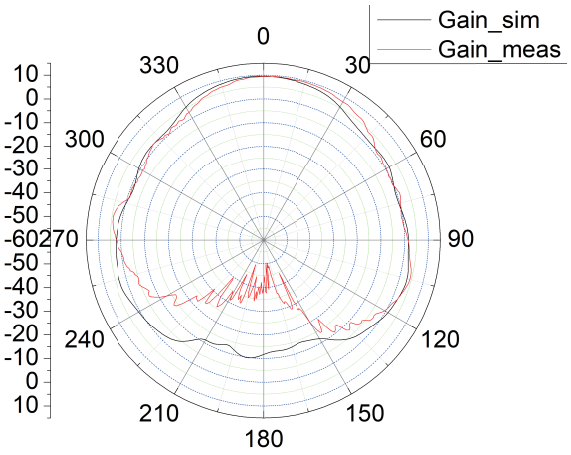

Figure 13. Gain in x-z plane of the 4-element end fire dipole antenna array.

proportional to geometric ratio, while the width and distances of neighboring dipoles in this work are constant, except that the outermost dipole is a half-wave dipole antenna. The architecture in this work is also expandable when N increases. In a word, this kind of end fire antenna array is characterized by high gain and simplicity in design (simplicity in structure and without matching networks), and has some research value.

5. CONCLUSION

N-element end fire antenna array could be constructed with $N-1$ elements of full wave dipole antennas and one half wave dipole antenna without additional impedance matching network. Three 24 GHz dipole end-fire antenna arrays: 2-element end-fire dipole antenna with gains of 7.1 dB, 3-element end-fire dipole antenna with gain of 8.4 dB, and 4-element end-fire dipole antenna with gain of 9.4 dB respectively are presented to explain and verify this end fire antenna architecture based on transmission line theory. This end-fire dipole antenna array composed of full-wave dipole antenna elements and half wave dipole antenna is characterized by high gain, compactness, and simplicity in design (simplicity in structure and without matching networks). This 24 GHz end-fire antenna architecture could be utilized in 24 GHz planar end-fire antenna arrays to increase the EIRP of the transmitter. This kind of antenna architecture is also applicable to other frequency bands such as on-chip planar mm-wave and THz antenna design.

ACKNOWLEDGMENT

The authors are thankful for Key Laboratory of RF Circuits and System Ministry of Education, School of Electronics and Information, Hangzhou Dianzi University, for measurements of S parameter, gain, and radiation pattern of the antennas.

REFERENCES

1. Shunshi, Z., *Antenna Theory and Techniques* , Publishing House of Electronic Industry, Beijing, 2015.
2. Yun, H. and K. Ma, "A cavity-backed end-fire dipole antenna using SISL technology for 24 GHz automotive anti-collision radar system," *In Proceedings of the 2018 IEEE MTT-S International Wireless Symposium (IWS)*, Chengdu, China, 2018.
3. Rajveer Singh, B., G. V. Rodney, and F. Mark, "Phased arrays and MIMO: Wideband 5G end fire elements on liquid crystal polymer for MIMO," *In Proceedings of the 2019 IEEE International Symposium on Phased Array System and Technology (PAST)*, Waltham, MA, USA, 2019.

4. Min, L., W. Rong, H. Yao, and W. Bo, "A low-profile wideband CP end-fire magnetoelectric antenna using dual-mode resonances," *IEEE Trans. Antennas Propagation*, No. 67, 4445–4452, 2019.
5. Li, A. and K. M. Luk, "Millimeter-wave end-fire magneto-electric dipole antenna and arrays with asymmetrical substrate integrated coaxial line feed," *IEEE Open J. Antennas Propagation*, No. 2, 62–67, 2021.
6. Zeng, J. and K. M. Luk, "Wideband millimeter-wave end-fire magnetoelectric dipole antenna with microstrip-line feed," *IEEE Trans. Antennas Propagation*, No. 68, 2658–2665, 2020.
7. Yanfei, M., E. Shiju, and Y. Suli, "A two-element 24 GHz planar end-fire dipole antenna array," *2021 International Applied Computational Electromagnetics Society (ACES-China) Symposium*, Chengdu, China, 2021.
8. Yanfei, M. and E. Shiju, "A 24 GHz end-fire helix antenna with high gain turn ratio in PCB technology," *2021 2020 IEEE MTT-S International Wireless Symposium (IWS)*, China, 2020.
9. Isbell, D. E., "Log periodic dipole arrays," *IRE Transactions on Antennas and Propagation*, Vol. 8, No. 3, 256–270, 1960.
10. Guohua, Z., C. Yong, Y. Qiuyan, Z. Shouzheng, and G. Jianjun, "Gain enhancement of printed log-periodic dipole array antenna using director cell," *IEEE Transactions on Antennas and Propagations*, Vol. 62, No. 11, 5915–5919, 2014.
11. Manekiya, M., R. Mendicino, V. Mulloni, M. Donelli, and G. Marchi, "A compact ultra-wide band printed log-periodic antenna using a bow-tie structure," *PIERS C*, Vol. 124, No. 52, 2022.
12. Azaro, R., F. G. B. De Natale, M. Donelli, A. Massa, and E. Zeni, "Optimized design of a multifunction/multiband antenna for automotive rescue systems," *IEEE Transactions on Antennas and Propagation*, Vol. 54, No. 2, 392–400, 2006.